Article

Design of an N-Methylated Peptide Inhibitor of #-Synuclein Aggregation Guided by Solid-State NMR

Jillian Madine, Andrew J. Doig, and David A. Middleton

J. Am. Chem. Soc., **2008**, 130 (25), 7873-7881 • DOI: 10.1021/ja075356q • Publication Date (Web): 30 May 2008

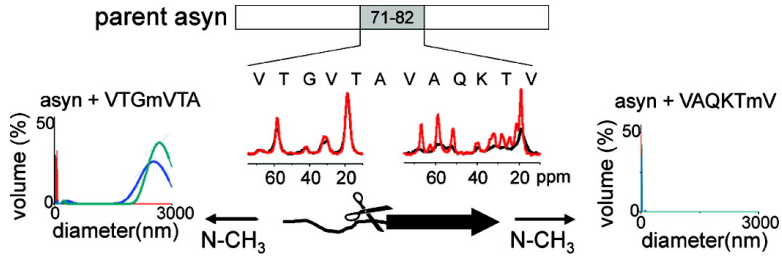

More About This Article

Additional resources and features associated with this article are available within the HTML version:

- Supporting Information
- Access to high resolution figures
- Links to articles and content related to this article
- Copyright permission to reproduce figures and/or text from this article

View the Full Text HTML

J|A|C|S
ARTICLES

Published on Web 05/30/2008

Design of an N-Methylated Peptide Inhibitor of α-Synuclein Aggregation Guided by Solid-State NMR[§]

Jillian Madine,[†] Andrew J. Doig,[‡] and David A. Middleton*,[†]

School of Biological Sciences, University of Liverpool, Crown Street, Liverpool L69 7ZB, United Kingdom, and Faculty of Life Sciences, Manchester Interdisciplinary Biocentre, University of Manchester, 131 Princess Street, Manchester M1 7DN, United Kingdom

Received July 18, 2007; E-mail: middleda@liv.ac.uk

Abstract: Many neurodegenerative diseases are associated with the aggregation of misfolded proteins into amyloid oligomers or fibrils that are deposited as pathological lesions within areas of the brain. An attractive therapeutic strategy for preventing or ameliorating amyloid formation is to identify agents that inhibit the onset or propagation of protein aggregation. Here we demonstrate how solid-state nuclear magnetic resonance (ssNMR) may be used to identify key residues within amyloidogenic protein sequences that may be targeted to inhibit the aggregation of the host protein. For α-synuclein, the major protein component of Lewy bodies associated with Parkinson's disease, we have used a combination of ssNMR and biochemical data to identify the key region for self-aggregation of the protein as residues 77−82 (VAQKTV). We used our new structural information to design a peptide derived from residues 77 to 82 of α-synuclein with an N-methyl group at the C-terminal residue, which was able to disrupt the aggregation of α-synuclein. Thus, we have shown how structural data obtained from ssNMR can guide the design of modified peptides for use as amyloid inhibitors, as a primary step toward developing therapeutic compounds for prevention and/or treatment of amyloid diseases.

Introduction

Many neurodegenerative diseases are associated with misfolded protein aggregation and deposition as pathological lesions in areas of the brain.[1] An attractive therapeutic strategy for preventing or ameliorating amyloid deposition in brain and other tissue is to identify agents that interfere with the fibril growth process, either by accelerating aggregation into benign insoluble deposits or by arresting the onset or propagation of fibril growth.[2] One approach that is gathering interest is to synthesize short peptides that correspond to a self-recognition element (SRE) of the native amyloid sequence but contain key modifications, so that the peptides bind to the parent protein at the SRE and prevent further aggregation.[3] Such modifications include β-sheet-breaking amino acid substitutions, addition of N- and C-terminal blocking groups, replacement of amide bonds with ester linkages, and introduction of α-disubstituted amino acids such as α-aminobutyric acid (reviewed in ref 3). A convenient and useful way to modify an SRE peptide is to introduce N-methylated backbone amide groups so that the peptide is unable to hydrogen-bond on one side. Doig and co-workers[4] first demonstrated this strategy for the β(25−35) fragment of β-amyloid, and it has subsequently been shown to be effective in inhibiting the aggregation of full-length β-amyloid[5−7] and amylin.[8] N-Methylation confers beneficial properties on the peptide in addition to acting as an aggregation inhibitor: the modified peptides are highly soluble in aqueous and organic solvents, resistant to proteolytic degradation, and diffuse across membranes.[6,9,10]

Lewy bodies are a form of neurodegenerative lesion having a dense core of insoluble filamentous proteins and lipids, surrounded by a peripheral halo. The major protein component of these inclusions is α-synuclein (asyn).[11] In aqueous solution asyn is predominantly unfolded,[12] but it can misfold into a state with a high propensity to aggregate into rigid, unbranched, 10

[§] Abbreviations: asyn, α-synuclein; CD, circular dichroism; CP-MAS, cross-polarization magic-angle spinning; CR, Congo red; DARR, dipolar assisted rotational resonance; DLS, dynamic light scattering; HFIP, hexafluoro-2-propanol; mA, *N*-methylalanine; mV, *N*-methylvaline; NAC, nonamyloid component; SRE, self-recognition element; ssNMR, solid-state nuclear magnetic resonance; ThT, thioflavin T.

[†] University of Liverpool.

[‡] University of Manchester.

(1) Murphy, R. M. *Annu. Rev. Biomed. Eng.* **2002**, *4*, 155–174.
(2) Gilead, S.; Gazit, E. *Angew. Chem., Int. Ed.* **2004**, *43* (31), 4041–4044.
(3) Sciarretta, K. L.; Gordon, D. J.; Meredith, S. C. *Methods Enzymol.* **2006**, *413*, 273–312.
(4) Hughes, E.; Burke, R. M.; Doig, A. J. *J. Biol. Chem.* **2000**, *275*, 25109–25515.
(5) Gordon, D. J.; Sciareta, K. L.; Meredith, S. C. *Biochemistry* **2001**, *40*, 8237–8245.
(6) Gordon, D. J.; Tappe, R.; Meredith, S. C. *J. Pept. Res.* **2002**, *60*, 34–55.
(7) Kokkoni, N.; Stott, K.; Amijee, H.; Mason, J. M.; Doig, A. J. *Biochemistry* **2006**, *45* (32), 9906–9918.
(8) Kapurniotu, A.; Schmauder, A.; Tenidis, K. *J. Mol. Biol.* **2002**, *315*, 339–350.
(9) Adessi, C.; Frossard, M.-J.; Boissard, C.; Fraga, S.; Bieler, S.; Ruckle, T.; Vilbois, F.; Robinson, S. M.; Mutter, M.; Banks, W. A.; Soto, C. *J. Biol. Chem.* **2003**, *278* (16), 13905–13911.
(10) Kokkoni, N.; Stott, K.; Amijee, H.; Mason, J. M.; Doig, A. J. *Biochemistry* **2006**, *45*, 9906–9918.
(11) Spillantini, L. C.; Schmidt, M. L.; Lee, V. M. Y.; Trojanowski, J. Q.; Jakes, R.; Goedert, M. *Nature* **1997**, *388*, 839–840.
(12) Weinreb, P. H.; Zhen, W.; Poon, A. W.; Conway, K. A.; Lansbury, P. T. J. *Biochemistry* **1996**, *35*, 13709–13715.

nm wide assemblies characteristic of amyloid fibrils.[13] Aggregation of asyn to form these insoluble fibrillar inclusions is a probable key event in the onset of many neurodegenerative diseases, including Parkinson's disease and the Lewy body variant of Alzheimer's disease. At present there are no methods available to prevent or cure these dementias, with treatments concentrating on improving symptoms.[14] The nature of the toxic species involved in disease is currently unclear, but it has been reported that asyn and asyn peptide fragments increase in neurotoxicity upon aggregation.[15] Previous studies have identified key regions within the asyn sequence that are necessary for aggregation of the protein. A central hydrophobic region (residues 61−95), identified as the nonamyloid component (NAC) of Alzheimer's disease plaques,[16] is believed to be responsible for aggregation, with various residues within the NAC region suggested as the key initiating sequence, including residues 66−74,[17] 68−78,[18] and 71−82.[19]

Information about the structural features of an amyloid species could help to identify SREs within asyn and other amyloidogenic proteins, which could serve as templates for modification to generate potential inhibitors. High-resolution solid-state nuclear magnetic resonance (ssNMR) is a powerful spectroscopic technique that can provide detailed structural information about proteins and peptides within amyloid fibrils and produce three-dimensional models of fibril architecture.[20] Recent notable examples formed by proteins and peptides include Aβ(1−40) in Alzheimer's disease,[21] transthyretin in senile systemic amyloidosis,[22] a peptide fragment of β_2-microglobulin,[23] and α-synuclein.[24] In the latter work, extensive assignment of the ^{13}C spectrum and chemical shifts analysis revealed that the sequence encompassing residues 38−95 forms the core fibrillar region, with turn regions identified as residues 66−68 and 83−86.

Solid-state NMR is beginning to attract attention as a potentially useful technique in the drug discovery process,[25] but so far there have been no reports, beyond well-characterized model systems, of how ssNMR has been exploited to generate, design, or optimize novel, pharmaceutically active lead compounds. Here, information provided by ssNMR has guided the rational design of a new N-methylated peptide that is effective as an inhibitor of asyn aggregation, thus providing a basis to develop drug candidates for neurodegenerative disease. We began by considering the peptide H_2N-VTGVTAVAQKTV-COOH, corresponding to residues 71−82 of full-length asyn. The peptide [asyn(71−82)] is a good starting point from which to develop N-methylated peptide inhibitors of asyn aggregation because (i) its residues constitute a critical SRE of native asyn[19] and are absent in β-synuclein, a nonaggregating homologue; (ii) the peptide alone readily aggregates to form insoluble amyloid fibrils of similar morphology to those of the parent protein;[26] and (iii) in the presence of full-length asyn, the peptide binds to and cofibrillizes with the aggregating parent protein.[19] Asyn(71−82) has seven residues (four valine, one glycine, and two alanine) at which to conveniently introduce one or more N-methyl groups via commercially available amino acid precursors. Ideally an inhibitor should only have N-methyl groups on one side to be able to bind to its target, giving the possibility of 22 ($=2^3 + 2^4 - 2$) variants to synthesize and test for their ability to bind to full-length asyn and inhibit aggregation. It is shown here that the number of possibilities for N-methylation can be reduced by using ssNMR to identify within the dodecameric peptide sequence the most critical sites for aggregation. By eliminating residues within asyn(71−82) that are unnecessary for aggregation, a small number of shorter N-methylated peptides have been prepared, one of which is shown to be effective in preventing asyn aggregation.

Experimental Section

Materials. Unenriched asyn(71−82) was synthesized in-house without terminal acetylation or amidation via solid-phase fmoc [*N*-(9-fluorenyl)methoxycarbonyl] L-amino acid chemistry, on an Activotec Apex peptide synthesizer. Cleavage from the resin was achieved with 95% trifluoroacetic acid and 5% water, and the peptide was precipitated and cleaned by ether washing. Purification was achieved by high-pressure liquid chromatography (HPLC) and the product identity and purity (over 95%) were confirmed by MALDI mass spectrometry. Four asyn(71−82) samples were also prepared with blocks of four contiguous amino acid residues (i.e., V^{71}TGV, V^{74}TAV, V^{77}AQK, and K^{80}TV) uniformly ^{13}C- and ^{15}N-enriched for NMR studies (Peptide−Protein Research Ltd.). Full-length asyn was purchased in solid form from rpeptide. The N-methylated peptides VmAQKTV, VAQKTmV, and VmAQKTmV were purchased in pure form without acetylation from Peptide−Protein Research Ltd.

Preparation of Peptides and Proteins for Aggregation Studies. Hexafluoro-2-propanol (HFIP) was added to all peptide samples tested to break up any preformed aggregated species present prior to initiation of aggregation studies. HFIP (1 mL) was added to 2 mg of lyophilized peptide, and the sample was vortexed to fully dissolve the material before it was sonicated at 25 °C for 5 min in a bath sonicator. HFIP was evaporated first under a stream of argon and then under high vacuum for 2 h. This process was repeated three times, followed by dissolution of the solid material in 3 mL of double-distilled H_2O, with thorough vortexing for 3 min.[27,28] The peptide was lyophilized ready for use.

Aqueous solutions of 450 μM asyn(71−82) or 70 μM full-length asyn were suspended in 10 mM phosphate, pH 7, and incubated with continuous agitation, at 37 °C. Samples were taken for analysis immediately after preparation of the solution and again at specified time points throughout the analysis for up to 6 weeks after the solution was prepared. In experiments to monitor the effect of N-methylated peptides on aggregation, aqueous samples of 70 μM full-length asyn or 450 μM asyn(71−82) were prepared with the N-methylated peptides present at equimolar concentrations and buffered to pH 7 with 10 mM phosphate. Samples were treated

(13) Conway, K. A.; Harper, J. D.; Lansbury, P. T. J. *Biochemistry* **2000**, *39*, 2552–2563.
(14) Stocchi, F. *Parkinsonism Relat. Disord.* **2003**, *9*, S73–S81.
(15) El Agnaf, O. M.; Jakes, R.; Curran, M. D.; Middleton, D.; Ingenito, R.; Bianchi, E.; Pessi, A.; Neill, D.; Wallace, A. *FEBS Lett.* **1998**, *440*, 71–75.
(16) Han, H.; Weinreb, P. H.; Lansbury, P. T. J. *Chem. Biol.* **1995**, *2*, 163–169.
(17) Du, H.; Tang, L.; Luo, X.; Li, H.; Hu, J.; Zhou, J.; Hu, H. *Biochemistry* **2003**, *42*, 8870–8878.
(18) Bodles, A. M.; Guthrie, D. J. S.; Greer, B.; Irvine, G. B. *J. Neurochem.* **2001**, *78*, 384–395.
(19) Giasson, B. I.; Murray, I. V. J.; Trojanowski, J. Q.; Lee, V. M. Y. *J. Biol. Chem.* **2001**, *276* (4), 2380–2386.
(20) Tycko, R. *Curr. Opin. Chem. Biol.* **2000**, *4*, 500–506.
(21) Petkova, A. T.; Ishii, Y.; Balbach, J. J.; Antzutkin, O. N.; Leapman, R. D.; Delaglio, F.; Tycko, R. *Proc. Natl. Acad. Sci. U.S.A.* **2002**, *99* (26), 16742–16747.
(22) Jaroniec, C. P.; MacPhee, C. E.; Astrof, N.; Dobson, C. M.; Griffin, R. G. *Proc. Natl. Acad. Sci. U.S.A.* **2002**, *99* (26), 16748–16753.
(23) Iwata, K.; Fujiwara, T.; Matsuki, Y.; Akutsu, H.; Takahashi, S.; Naiki, H.; Goto, Y. *Proc. Natl. Acad. Sci. U.S.A.* **2006**, *103*, 18119–18124.
(24) Heise, H.; Hoyer, W.; Becker, S.; Andronesi, O. C.; Riedel, D.; Baldus, M. *Proc. Natl. Acad. Sci. U.S.A.* **2005**, *102* (44), 15871–15876.
(25) Watts, A. *Nat. Rev. Drug Discovery* **2005**, *4* (7), 555–568.
(26) Madine, J.; Doig, A. J.; Middleton, D. *Biochem. Soc. Trans.* **2005**, *33* (5), 1113–1115.
(27) Srinivasan, R.; Jones, E. M.; Liu, K.; Ghiso, J.; Marchant, R. E.; Zagorski, M. G. *J. Mol. Biol.* **2003**, *333*, 1003–1023.
(28) Chen, S.; Wetzel, R. *Protein Sci.* **2000**, *10*, 887–891.

with HFIP and sonication prior to mixing, as described above, and incubated at 37 °C with agitation.

Analysis of Aggregation. Dynamic light scattering (DLS) was used to study the rate of aggregation of full-length and peptide fragments of asyn, and to identify any increase in size of peptide species present over time, possibly representing aggregation intermediates along the fibrillization pathway. Peptide (50 μL in 10 mM phosphate, pH 7) was added to a 3 mm cell. A series of 20 measurements of 10 s each were taken at 30 °C on a Zetasizer Nano DLS machine from Malvern Instruments, and averaged profiles were produced. Samples were incubated in 10 mM phosphate buffer, pH 7, at 37 °C, with agitation and readings repeated.

Aggregation of full-length asyn and peptide fragments was also monitored with the fluorescent dyes thioflavin T (ThT) and Congo red (CR). ThT binds to aggregated amyloid, causing a change in absorbance values of its excitation and emission spectra.[29] Peptide sample (43.0 μL) was added to 2.96 mL of 10 μM ThT (Sigma) in 10 mM Tris, pH 7.5; the mixture was vortexed and transferred to a 1 cm path length cuvette. Spectra were recorded on a Cary Eclipse Varian fluorescence spectrophotometer with excitation at 450 nm and emission at 482 nm with band-pass 5 nm. A new excitation peak at 450 nm and enhanced emission at 482 nm are observed when amyloid is present. For analysis by CR, peptide samples (75.0 μL) were added to 675 μL of 200 μM CR solution (Sigma) in 5 mM potassium phosphate and 0.15 M sodium chloride, pH 7.4; the mixtures were vortexed and left at room temperature for 30 min. Readings were then taken on a Cary 300 Bio UV−visible spectrophotometer at 480 and 540 nm with a blank of CR (200 μM). The amount of CR bound was calculated from

$$\mathrm{CR}_{\mathrm{bound}} = \frac{\left(\frac{A_{540}}{\varepsilon_{\mathrm{bound}}}\right) - \left(\frac{A_{480}}{\varepsilon_{\mathrm{unbound}}}\right)}{l} \quad (1)$$

where $\varepsilon_{\mathrm{bound}}$ is 2.53×10^5 M^{-1} cm^{-1} (the molar extinction coefficient of bound CR), $\varepsilon_{\mathrm{unbound}}$ is 4.63×10^5 M^{-1} cm^{-1} (the molar extinction coefficient of unbound CR), and l is the path length in centimeters. The concentration of CR bound is expressed in molar units.

The amount of insoluble material formed by aggregation of the asyn peptides was quantified by sedimentation. Following incubation for 1 week at 37 °C with agitation, insoluble aggregates were removed by centrifugation at 13 000 rpm (18900*g*) in a Sigma 15K4 centrifuge for 1 h. The amount of peptide remaining in the supernatant was analyzed after alkaline hydrolysis by use of the primary amine-reactive agent ninhydrin.[30]

Far-UV circular dichroism (CD) spectra were recorded on a Jasco J-810 spectropolarimeter at 25 °C. Spectra were recorded over the 250−190 nm range at a scan rate of 10 nm/min with step size of 0.1 nm. Spectra were recorded as the average of four scans. Peptide (20 μM in 10 mM phosphate, pH 7.4) was added to a 0.1 cm cuvette. After the spectra were recorded, spectral amplitudes were converted to molar elipticity values (θ) after subtractiion of control spectra according to

$$\theta = \frac{\mathrm{CD}}{10\mathrm{cln}} \quad (2)$$

where CD is the spectral amplitude (millidegrees), c is the peptide concentration (molar), l is the path length (centimeters), and n is the number of amino acids.

Morphologies of the insoluble aggregates of asyn(71−82) and asyn formed following incubation were analyzed by electron microscopy via negative staining methods (4% uranyl acetate). Peptide suspensions (10 μL) were loaded onto carbon-coated copper grids and visualized on a Tecnai 10 electron microscope at 100 kV. Images were printed onto photographic paper.

Sample Preparation for NMR. Following treatment to remove any preformed fibrils or protofibrils, 5 mg of each uniformly ^{13}C- and ^{15}N-enriched soluble asyn(71−82) in turn was dissolved in 80 μL of 10 mM phosphate buffer, pH 7, and transferred to a 4 mm diameter zirconium rotor. Aqueous solutions of 2 mM of each asyn(71−82), uniformly ^{13}C- and ^{15}N-enriched, were incubated in 10 mM phosphate, pH 7, with continuous agitation, at 37 °C, for up to 6 weeks. Insoluble fibrillar species were separated by centrifugation at 13 000 rpm for 30 min and then transferred to a 4 mm rotor, and ^{13}C CP-MAS spectra were produced. The supernatant was also transferred to a rotor and spectra were produced. HCl or NaOH (1 M) was added to peptide samples within the rotor, and they were vortexed until the required pH was reached. The pH value was confirmed with a micro pH probe. For NMR experiments at −10 °C the samples were flash-frozen by immersing the rotor in liquid nitrogen and then the rotor was transferred immediately to the precooled NMR probe head. The samples were not allowed to thaw until all NMR experiments were completed.

NMR Experiments. NMR experiments were performed on a Bruker Avance 400 spectrometer operating at a magnetic field of 9.3 T. The spinning rate was maintained automatically at 8 kHz ± 1 Hz. Typical conditions for CP-MAS experiments were a ^{1}H 90° excitation pulse length of 4.0 μs, Hartmann−Hahn cross-polarization from ^{1}H to ^{13}C at a contact times of 1−5 ms with a matched ^{1}H field of 65 kHz, continuous wave proton decoupling at a field of 85 kHz during signal acquisition, and a 2-s recycle delay. Two-dimensional dipolar assisted rotational resonance (DARR) spectra[31] were recorded with 128 hypercomplex points in the indirect dimension with 256 scans/increment and a mixing time of 50 ms, during which the proton field was adjusted to the spinning frequency of 8 kHz. The total acquisition time for each DARR experiment was 19 h. Experiments were conducted at −10 °C to eliminate dynamics that could scale or eliminate the dipolar couplings that are required for magnetization transfer.

Results and Discussion

Secondary structure analysis of asyn(71−82) and full-length asyn by CD agreed with previous observations[19,26] that both are in the predominantly random coil form associated with their monomeric states, but over a period of days both adopt β-sheet characteristics consistent with the conformational changes that are usually required for aggregation of peptides and proteins into amyloid fibrils (Figure 1a,b). Analysis of the asyn(71−82) aggregates by electron microscopy revealed an amyloid-like fibril morphology similar to that of asyn aggregates (Figure 1c), in agreement with earlier observations of this peptide.[32]

High-resolution ^{13}C ssNMR was next used to examine in greater detail how the structure of asyn(71−82) differs before and after aggregation, to specify which amino acid residues undergo a transformation from the disordered, random state into the highly ordered β-sheet conformation associated with β-amyloid. The degree of change in structural order along the asyn(71−82) sequence associated with aggregation could then be used to produce an amyloidogenicity profile to help identify the most amyloidogenic residues that could be targeted for N-methylation in the design of asyn aggregation inhibitors. Site-specific structural information about monomeric, soluble asyn(71−82) and insoluble fibrils was obtained from measurements of peak widths and chemical shifts from two-dimensional ^{13}C DARR spectra of the peptide monomer in aqueous solution

(29) Levine, H. *Protein Sci.* **1993**, *2*, 404–410.
(30) Rosen, H. *Arch. Biochem. Biophys.* **1957**, *67*, 1–15.
(31) Takegoshi, K.; Nakamura, S.; Terao, T *Chem. Phys. Lett.* **2001**, *344*, 631–637.
(32) Serpell, L. C.; Berriman, J.; Jakes, R.; Goedert, M.; Crowther, R. A. *Proc. Natl. Acad. Sci. U.S.A.* **2000**, *97* (9), 4897–4902.

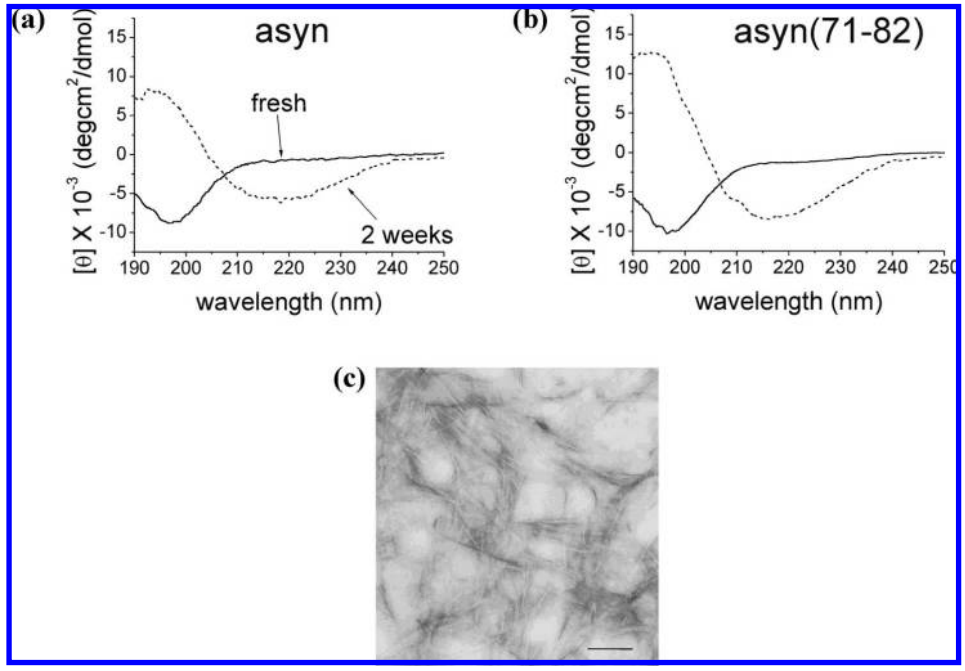

Figure 1. CD spectra of (a) asyn and (b) asyn(71−82): (—) freshly prepared and (---) after incubation in 10 mM phosphate buffer, pH 7, 37 °C, with agitation for 2 weeks. (c) Electron micrograph of negatively stained fibrils formed following incubation of 450 μM asyn(71−82) in 10 mM phosphate buffer, pH 7, at 37 °C for 2 weeks; scale bar 100 nm.

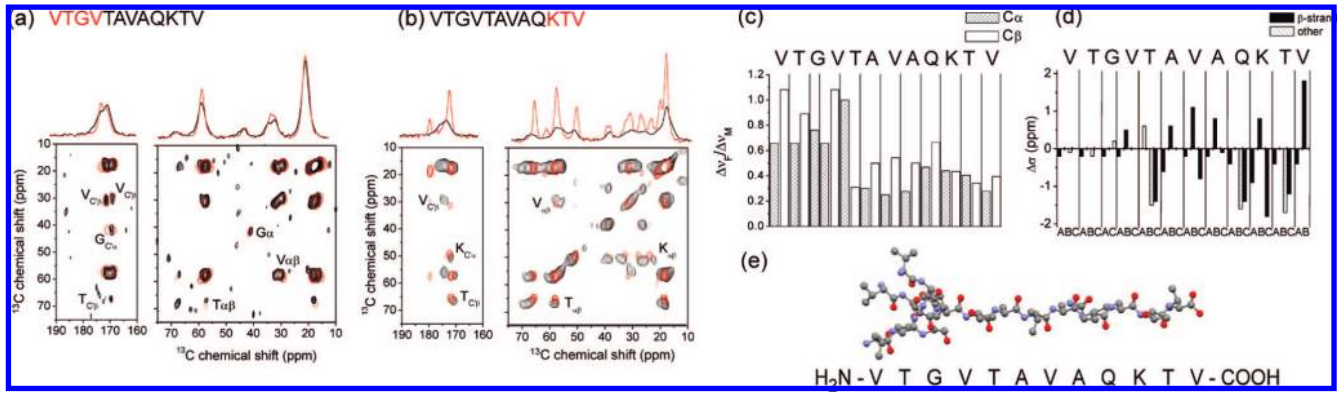

Figure 2. High-resolution ^{13}C ssNMR analysis of asyn(71−82) in monomeric form in aqueous solution and as an aqueous suspension of insoluble fibrils. DARR spectra and peak assignments for asyn(71−82) uniformly ^{15}N- and ^{13}C-enriched either at residues (a) V^{71}TGV or (b) K^{80}TV are shown for the monomer (black) and fibril (red) samples. The corresponding one-dimensional spectra for the monomer and fibrils are shown at the top. Sequence-specific changes in (c) ^{13}C peak widths and (d) chemical shifts for (A) Cα, (B) Cβ, and (C) backbone carbonyl sites accompanying the aggregation of monomeric asyn(71−82) into insoluble fibrils were measured from the DARR spectra shown and from spectra of asyn(71−82) monomers and fibrils ^{13}C/^{15}N-enriched at V^{74}TAV and V^{77}AQK (not presented). Changes in chemical shift values are expressed as $\Delta\sigma = \sigma$(monomer) − σ(fibril), and those changes consistent with a random coil−β-strand transition are represented as black bars. Changes in peak widths at half-height for carbonyl, Cα, and Cβ sites are expressed as the ratio of fibril peak widths to monomer peaks widths ($\delta\nu_M$). (e) Model of asyn(71−82) with an ordered β-strand conformation at the C-terminus and a disordered N-terminus, consistent with the NMR data. Spectra were obtained from 5 mg of monomeric peptide freshly prepared in an aqueous solution of 80 μL of 10 mM phosphate buffer, pH 7 (black), and from a suspension of fibrils (approximately 2 mM) in the same buffer solution (red).

at −10 °C and then, at the same temperature, for an aqueous suspension of fibrils formed after 4 weeks of incubation. Block labeling of three or four consecutive amino acids[22] was employed to reduce crowding in the spectrum and simplify analysis. Each block overlapped by one residue to confirm that there was no structural variation between samples. The DARR spectra for the N- and C-terminally enriched peptides before and after aggregation are shown with assignments in Figure 2a,b. Spectra of the monomeric species exhibited uniformly broad peaks across the entire sequence, consistent with a disordered, structurally heterogeneous peptide distribution in the frozen solution. The spectra of the peptides after aggregation suggested a differential change in structural order along the sequence, with peaks for the N-terminal residues remaining broad and peaks for the C-terminal residues narrowing substantially. The changes in line widths at half-height ($\delta\nu$) for Cα and Cβ sites across the peptide sequence are consistent with an increase in the structural order of residues progressing from the N-terminus to the C-terminus (Figure 2c). Similarly, measurements of ^{13}C chemical shifts for carbonyl, Cα, and Cβ sites before and after aggregation of the peptide show the largest changes in shift values occur for the C-terminal residues, with little or no change in the values for the N-terminal residues (Figure 2d). The chemical shift differences are mostly consistent with a random

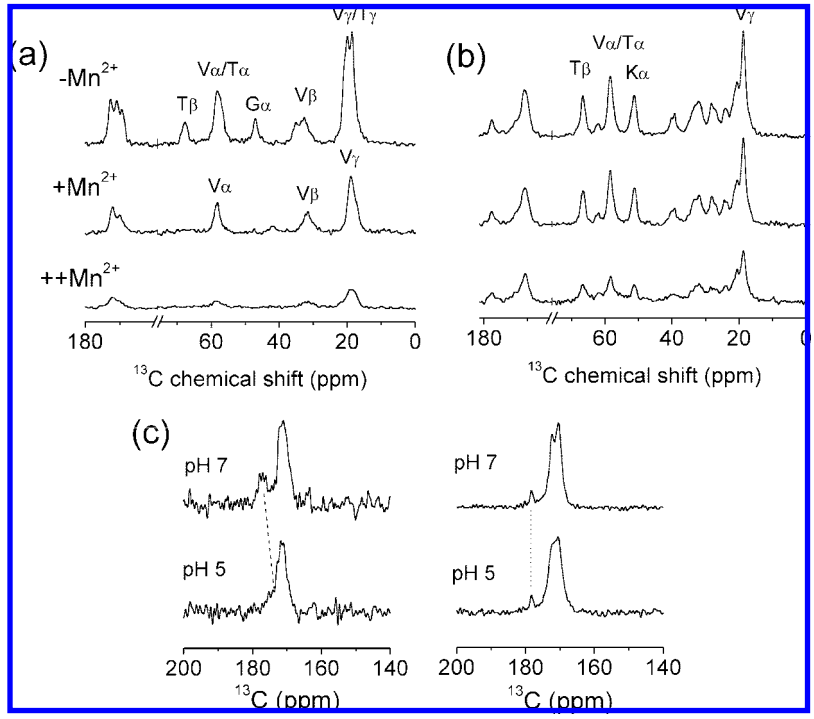

Figure 3. ^{13}C CP-MAS experiments to probe exposed and buried residues in fibrils of asyn(71−82). Monomeric peptide (2 mM) was freshly prepared in an aqueous solution of 10 mM phosphate buffer, pH 7, and fibrils were suspended in the same buffer solution. Spectra are shown for aqueous fibril suspensions of asyn(71−82) uniformly ^{15}N and ^{13}C enriched at residues (a) $V^{71}TGV$ and (b) $K^{80}TV$. Spectra were acquired before the addition of $MnCl_2$ ($-Mn^{2+}$) and after the addition of $MnCl_2$ to a concentration of 20 μM ($+Mn^{2+}$) and 40 μM ($++Mn^{2+}$). (c) Carbonyl ^{13}C peaks for asyn(71−82) labeled at $K^{80}TV$ are shown for 2 mM monomeric peptide in frozen aqueous solution (left) and for fibrils (right) at pH 5 and 7. The position of the peak for the terminal carboxyl carbon is denoted by the dotted line.

coil to β-sheet conformational change,[33] with the exception of the Thr81 and Gln79 Cβ sites. As these are both polar residues, the chemical shift differences may be dominated by the effects of intermolecular hydrogen bonding between the side chains of a single β-sheet or perhaps within an intersheet space. The spectra are thus consistent with the C-terminal residues of asyn(71−82) adopting a highly ordered β-strand conformation in the fibrils, whereas the N-terminal residues $V^{71}TGVT$ remain essentially as disordered as in the monomeric peptide (Figure 2e).

Further ^{13}C experiments were carried out on an aqueous suspension of the fully formed fibrils to identify exposed and buried amino acid residues according to their accessibility to paramagnetic Mn^{2+}. Regions of the fibrils that are exposed to Mn^{2+} in the aqueous environment are expected to undergo enhanced transverse relaxation rates,[34] which will be manifest in the ^{13}C spectrum as a loss of peak intensity or line broadening, whereas regions within buried regions will be affected less by Mn^{2+}. The ^{13}C CP-MAS NMR spectra of fibrils of the N- and C-terminally block-labeled peptides are shown in Figure 3a,b. In the spectra of $V^{71}TGV$-labeled fibrils, peaks for Gly and Thr are abolished after the addition of 20 μM Mn^{2+}, leaving peaks for Val that are diminished in intensity (e.g., by ~50% for Vβ) relative to the original spectrum (Figure 3a). Although it was not possible to assign the remaining peaks to either V^{71} or V^{74}, it is reasonable to suggest that the remaining peaks are from V^{74} rather than from V^{71} because the N-terminal residue is more likely to resemble T^{72} and G^{73}in terms of its accessibility to Mn^{2+}. In any case, further addition of Mn^{2+} to 40 μM virtually abolishes the remaining peaks, suggesting that V^{74}, too, is influenced by Mn^{2+} at the higher concentration of the metal ion. By contrast, the peaks for the $K^{80}TV$-labeled fibrils remain virtually unchanged after addition of 20 μM Mn^{2+} and diminish only by ~50% after further addition of Mn^{2+} (Figure 3b). These results suggest that the disordered N-terminal residues of peptides within the fibrils are more exposed to the external aqueous environment than are the C-terminal residues, which may be buried within an ordered β-sheet amyloid core. Further evidence that the C-terminal residues are excluded from the external environment of the fibrils was provided by monitoring the chemical shift for the C-terminal Val carboxyl carbon over a pH titration (Figure 3c). In the spectrum of a frozen solution of $K^{80}TV$-enriched monomeric peptide, the carboxyl peak is distinct from the other peaks at pH 7, but at pH 5 the peak moves upfield where it becomes partially overlapped by the other carboxyl peaks. This chemical shift change is consistent with a shift in the equilibrium of the carboxyl group toward its protonated state as the pH approaches the carboxyl pK_a. In the spectrum of the same peptide but in fibril form, the Val carboxyl peak is again distinct from the other peaks at pH 7, but when the pH is lowered the peak remains at the same chemical shift. Such a lack of an effect is consistent with the C-terminal carboxyl group sensing a constant pH of its local milieu and being excluded from the pH changes occurring in the external aqueous environment.

The results of the NMR experiments suggest that the C-terminal residues of asyn(71−82) play a predominant role in the fibrillization process whereas the N-terminal residues contribute less toward aggregation or are redundant. To confirm the fibrillogenic potential of these two regions, studies were

(33) Wang, Y.; Jardetzky, O. *Protein Sci.* **2002**, *11*, 852–861.
(34) Grobner, G.; Glaubitz, C.; Watts, A. *J. Magn. Reson.* **1999**, *141* (2), 335–339.

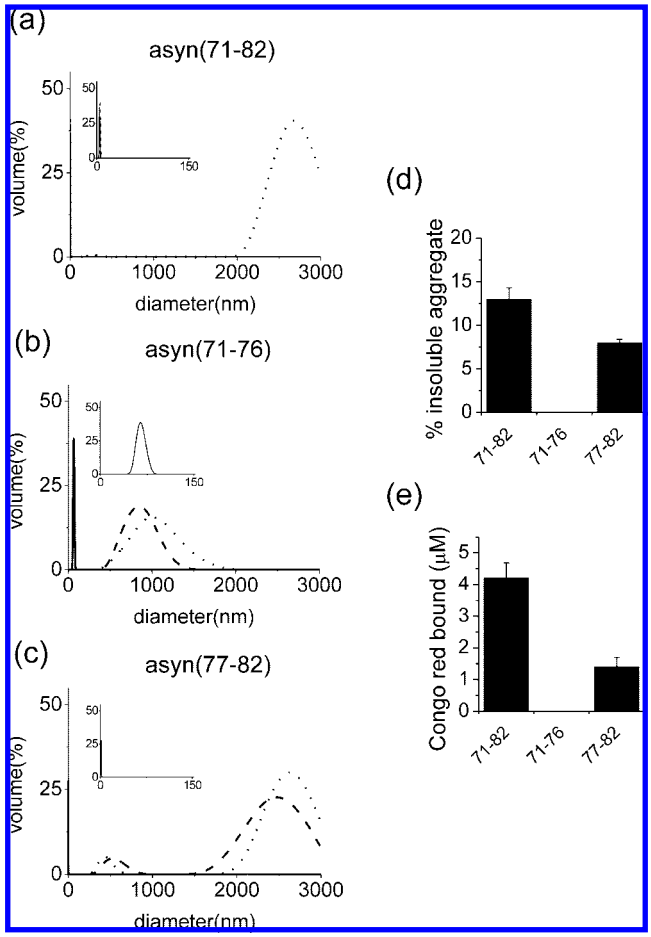

Figure 4. Analysis of the aggregation of asyn peptide fragments. Profiles of peptide size distributions obtained by DLS are shown for (a) asyn(71−82), (b) asyn(71−76), and (c) asyn(77−82). The size of the individual peptide species present are represented as the percentage volume of the total size distribution in the solution. Data are shown for freshly prepared samples (—) and for samples incubated for 1 week (---) and 2 weeks (•••). Insets show the region from 0 to 150 nm in more detail. The initial peptide concentration was 450 μM. (d) Amount of insoluble aggregated material in the sample, estimated from the concentration of peptide remaining in the supernatant after ultracentrifugation. (e) Amyloid content of each peptide solutions after incubation for 7 days, analyzed by binding of the amyloid diagnostic agent Congo red.

conducted to compare the rates of aggregation of asyn(71−82) with the truncated analogues asyn(71−76), containing the disordered N-terminal residues VGTVTA, and asyn(77−82), containing only the ordered C-terminal residues VAQKTV. Peptide aggregation was monitored for up to 2 weeks after the peptides were dissolved in aqueous solution to a concentration of 450 μM. DLS was used to follow the aggregation process by identifying the hydrodynamic diameter of the major peptide species present initially and after 1 or 2 weeks of incubation at 37 °C. DLS was chosen to follow the aggregation process as it has been shown to be suitable for the detection of intermediate species on the fibril formation pathway of amyloidogenic proteins/peptides.[35] In the case of asyn(71−82), no change was observed in the size of the initial species after 1 week of incubation. After 2 weeks, a new species of asyn(71−82) had formed, characterized by a diameter of greater than 2000 nm (Figure 4a). Hence a substantial lag phase exists before fibril nucleation and maturation. At the 2-week end point, asyn(71−82) had formed insoluble aggregates that could be isolated from solution by centrifugation (Figure 4d) and also bound the amyloid diagnostic dye CR (Figure 4e). The peptide asyn(71−76) aggregated after 1 week to form intermediate-size species of diameter less than 1000 nm (Figure 4b). No larger species were formed after a further week of aggregation. At the end point no insoluble material could be isolated by centrifugation (Figure 4d) and no amyloid species could be detected by CR binding (Figure 4e) or by electron microscopy (data not presented). By contrast, asyn(77−82) clearly aggregated after only 1 week to produce a mixture of intermediate size (∼500 nm) and large (>2000 nm) species (Figure 4c), which remained present in the solution after a further week of incubation. Insoluble aggregated material could be isolated from the asyn(77−82) solution by centrifugation (Figure 4d), and the presence of amyloid species could be detected by CR binding (Figure 4e). Hence, truncation of the N-terminal residues of asyn(71−82) accelerates aggregation into amyloid species, whereas the six N-terminal residues form smaller soluble aggregates that do not have the characteristics of amyloid. These results thereby provide further evidence that the C-terminal end of asyn(71−82), comprising residues V^{77} AQKTV, represents the critical region for forming ordered fibrils.

In view of the enhanced aggregation properties of asyn(77−82), N-methylated derivatives of this short peptide were prepared in order to test their effectiveness as inhibitors of full-length asyn aggregation. We examined three modified peptides having the alanine and/or valine residues of asyn(77−82) replaced by *N*-methylalanine (mA) and *N*-methylvaline (mV). For comparison, two N-methylated derivatives of asyn(71−76) were also prepared. Since asyn(71−76) exhibits a lower propensity to aggregate than does asyn(77−82), and thus does not contain a strong SRE, it is predicted that N-methylation of this peptide will not yield effective inhibitors of full-length asyn aggregation. The peptides mVTGVTA and VTGmVTA, derived from asyn(71−76), and VmAQKTV, VAQKTmV, and VmAQKTmV, derived from asyn(77−82), were first examined alone to determine whether N-methylation reduced their propensity to self-associate. It is desirable for the peptides to be stable as low molecular weight species, ideally monomeric, in order for them to bind to asyn and inhibit aggregation. DLS measurements of the three peptides over a 2-week period revealed that they have different aggregation characteristics. For VmAQKTV, a small increase in hydrodynamic diameter was observed after 1 week, forming a species with an average size of approximately 250 nm, but no larger species were observed after a further week of incubation (Figure 5c). The peptides mVTGVTA, VTGmVTA and VAQKTmV did not increase markedly in size over the 2-week time period compared to the parent peptides (Figure 5a, b, and d). Hence, substituting N-methyl groups into single alanine or valine residues reduces the aggregation potential of the modified peptides compared to that of asyn(71−76) and asyn(77−82). The double-methylated peptide VmAQKTmV showed the greatest increase in size, forming a species of approximately 1000 nm after incubation for two weeks (Figure 5e, •••). This large species did not bind the diagnostic dyes CR and ThT and thus may comprise nonamyloid aggregates formed as a consequence of the increased hydrophobicity conferred by the two additional methyl groups. This peptide was therefore considered unsuitable as an inhibitor of asyn aggregation and was not examined further.

(35) Walsh, D. M.; Lomakin, A.; Benedek, G. B.; Condron, M. M.; Teplow, D. B. *J. Biol. Chem.* **1997**, *272* (35), 22364–22372.

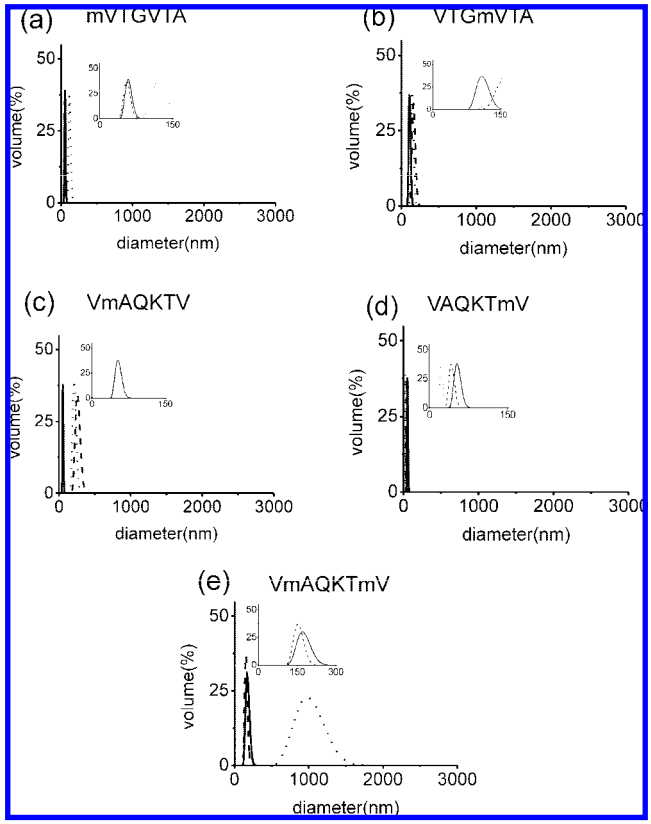

Figure 5. DLS analysis of the aggregation of the N-methylated peptides (a) mVTGVTA and (b) VTGmVTA, derived from asyn(71−76), and (c) VmAQKTV, (d) VAQKTmV, and (e) VmAQKTmV, derived from asyn(77−82). The size of the individual peptide species present are represented as the percentage volume of the total size distribution in the solution. Data are shown for freshly prepared samples (—) and for samples incubated for 1 week (---) and 2 weeks (•••). Insets show the region from 0 to 150 nm in more detail.

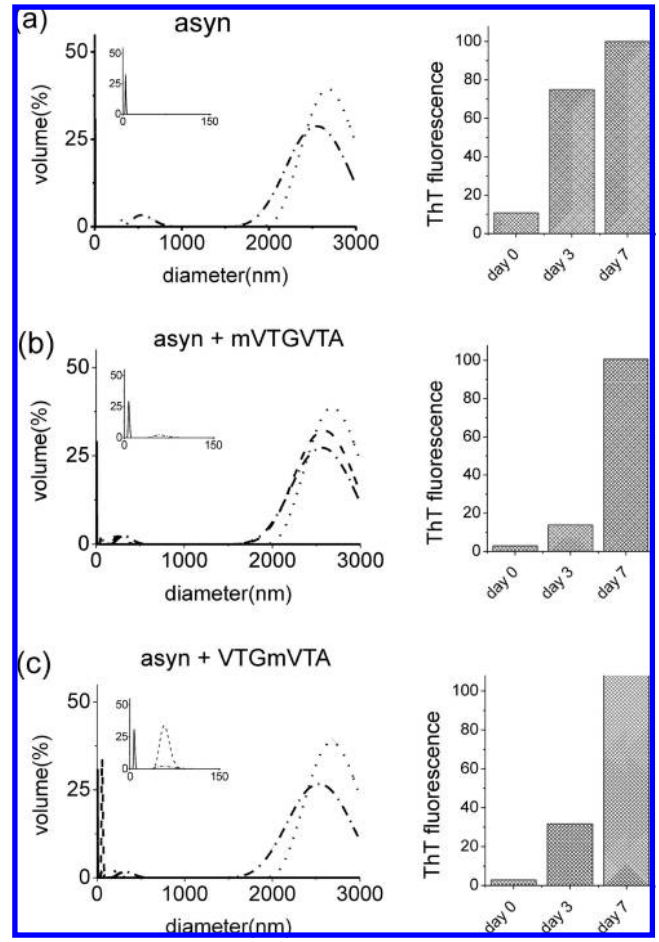

Figure 6. Analysis of the aggregation of 70 μM asyn in aqueous buffer solution, alone and in the presence of N-methylated peptides derived from asyn(71−76). The progression of aggregation was monitored by DLS (left) and by measuring ThT fluorescence (right) for asyn alone (a) and in the presence of an equimolar concentration of (b) mVTGVTA or (c) VTGmVTA. DLS data are shown for freshly prepared samples (—) and for samples incubated for 2 days (---), 4 days (-•-), and 7 days (•••). Insets show the region from 0 to 150 nm in more detail. Fluorescence values are shown for freshly prepared samples and samples incubated for 3 and 7 days, and all measurements are expressed as a percentage of fluorescence for asyn alone at day 7.

The four peptides mVTGVTA, VTGmVTA, VmAQKTV, and VAQKTmV were examined for their effects on asyn aggregation by a combination of DLS, ThT binding analysis, and electron microscopy. Full-length asyn was incubated at 37 °C with agitation and the aggregation process was studied over 1 week. This time period was chosen to allow asyn to aggregate to completion, culminating in the formation of large insoluble fibrils, so that changes in aggregation rate and the size and morphology of the end-point species upon coincubation with the peptides could be easily analyzed. In the absence of N-methylated peptides, DLS revealed that small species of asyn (approximately 10 nm), consistent with monomeric protein, appeared initially and after 2 days, but no evidence of larger species was found (Figure 6a, left, — and ---). After incubation for 4 days, asyn aggregated to form a mixture of intermediate and large species with mean sizes of approximately 500 and 2500 nm (Figure 6a, left, -•-). Further incubation appeared to reduce the amount of intermediate aggregates, leaving the predominantly larger species (Figure 6a, left, •••). ThT fluorescence measurements showed a progressive increase in the level of ThT binding to asyn incubated alone, indicating an increase in amyloid formation over the 7 day time period (Figure 6a, right). A similar distribution of high molecular weight species and similar changes in ThT fluorescence were observed when asyn was incubated in the presence of mVTGVTA (Figure 6b) and VTGmVTA (Figure 6c). DLS analysis of asyn in the presence of mVTGVTA suggested that the aggregation rate increased (in comparison to asyn incubated alone) after 2 days, forming a mixture of large aggregates comparable in size to those formed by incubation of asyn alone after 4 days (i.e., approximately 500 nm and 2000−3000 nm) (Figure 6b, ---). The ThT data for this peptide indicated less aggregation at day 3, however, suggesting that these aggregation intermediates may bind ThT more weakly. In any event, neither of the peptides derived from asyn(71−76) impeded asyn aggregation after 7 days, consistent with the VTGVTA sequence being a weak SRE as predicted from the NMR experiments.

DLS analysis of the two singly methylated derivatives of asyn(77−82) indicated that VmAQKTV did not prevent asyn aggregation (Figure 7a). Crucially, the other peptide, VAQKTmV, had a considerable inhibitory effect on the aggregation of asyn, preventing formation of the intermediate and large species observed for the protein alone or with VmAQKTV over the time period studied (Figure 7b). In the presence of VAQKTmV, no increase in the size of asyn was observed within the first 2 and 4 days, respectively (Figure 7b, inset), but after 7 days the size increased to approximately 50 nm, which could be attributed to dimers or trimers of asyn or to aggregates of

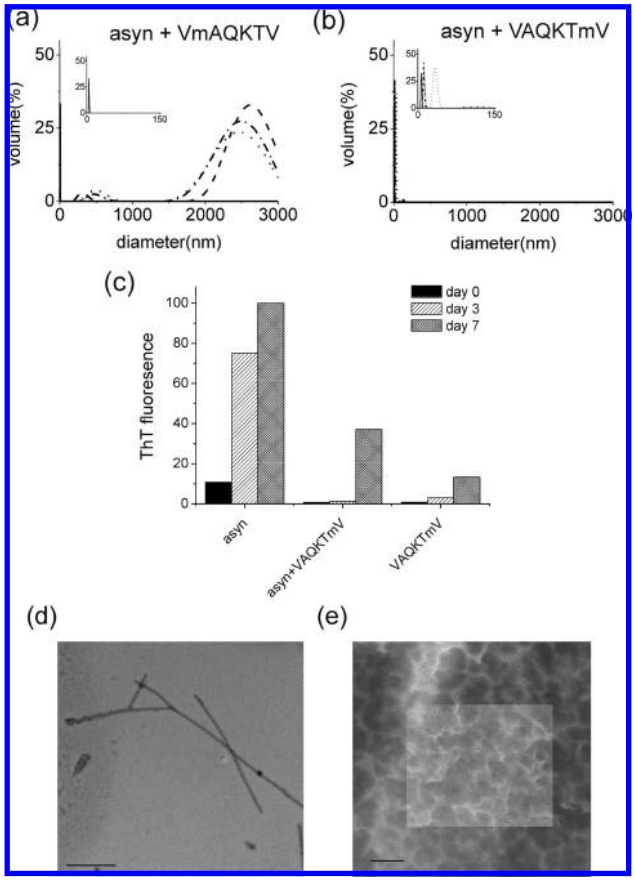

Figure 7. Analysis of the aggregation of 70 μM asyn in aqueous buffer solution, alone and in the presence of N-methylated peptides derived from asyn(77−82). DLS data are shown for asyn with an equimolar concentration of (a) VmAQKTV or (b) VAQKTmV prepared fresh (—) or incubated for 2 days (---), 4 days (-•-), and 7 days (•••). (c) ThT fluorescence values for asyn alone, asyn with VAQKTmV, and VAQKTmV alone. (d, e) Electron micrographs at the day 7 end point for (d) asyn alone and (e) asyn in the presence of VmAQKTV; scale bar 100 nm. Fluorescence values are expressed as a percentage of fluorescence for asyn alone at day 7. The time points for the DLS and ThT measurements are as described for Figure 6.

methylated peptide alone (Figure 5d, inset). Analysis of asyn aggregation by ThT indicated that when VAQKTmV was present in the incubation solution, no increase in ThT fluorescence was observed until day 7 (Figure 7c), when approximately 40% of the ThT fluorescence intensity for asyn alone was observed. However, incubation of VAQKTmV alone also showed a small increase in ThT intensity (~20% of wild-type signal) indicating that the 50 nm aggregates observed at day 7 by DLS could be partially due to aggregation of VAQKTmV alone. Electron microscopic analysis of aggregates formed by asyn alone after 7 days confirmed the presence of a dense network of insoluble fibrillar species characteristic of amyloid fibrils (Figure 7d). Electron microscopic analysis of asyn coincubated with VmAQKTV for 7 days revealed fewer structures, usually present as individual flexible fibrils, which are thinner and shorter, and approximately 200 nm in length (Figure 7e). There are no visible structures observed by electron microscopy when asyn is incubated in the presence of VAQKTmV for 7 days (data not presented).

In summary, one of three N-methylated peptides derived from the critical C-terminal residues of asyn(71−82) is highly effective at inhibiting the aggregation of asyn, whereas, as expected from the SSNMR analysis, asyn aggregation is not impeded by either of the two peptides derived from the redundant N-terminal residues of asyn(71−82). As is common in drug discovery, the probability of a modified peptide being active as an aggregation inhibitor is inherently low because the effectiveness of the peptide depends not only upon it having a high affinity for the SRE of the target but also on it having a low propensity to self-associate or to interact with the target nonspecifically at other sites, which can in some cases promote aggregation of the target protein. For example, in the search for peptide inhibitors of polyglutamine aggregation, Nagai et al.[36] screened 2.5×10^{11} phage from a random peptide phage display library to isolate 350 peptides, of which just six were effective as inhibitors. Solid-state NMR can, as shown here, increase the probability of identifying a hit by predicting N-methylated peptide sequences most likely to bind to the SRE of the target, but the aggregation properties of the modified peptide must still be verified experimentally. It is not clear why VmAQKTV is less effective than VAQKTmV, although it is possible that the partial aggregation of VmAQKTV alone to form small (250 nm) species within 1 week (Figure 5c) may render the peptide inactive. Our recent work has also shown that replacing alanine in asyn(77−82) with other nonnatural amino acids does produce effective inhibitors (unpublished results). It should therefore be noted that, although this work has focused on N-methylated peptides, the structure-based approach demonstrated here can be used in conjunction with any of the classes of modified peptides that have been shown to inhibit amyloid formation.

Conclusions

This work has demonstrated the benefit of using structural information to assist in the design of short peptides modified from the native sequence of amyloidogenic proteins for use in developing disease-modifying agents for use as therapeutics. Several techniques exist for probing the architecture of amyloid fibrils at the atomic level. Hydrogen/deuterium (H/D) exchange is one successful approach that has been used to identify β-sheet cores within amyloid fibrils.[37–39] The preformed fibrils are washed in D_2O so as to allow the exposed backbone amide protons to be exchanged for deuterium. The fibrils may then be dissolved in an aprotic solvent such as dimethyl sulfoxide, and solution NMR or mass spectroscopy is used to identify which regions are least susceptible to deuterium exchange, such as those within hydrogen-bonded β-sheets. In the context of the work here, this approach is useful for identifying self-recognition elements within large amyloidogenic proteins that could be targeted by inhibitors. Solid-state NMR is a valuable complementary technique that offers the advantage of being able to probe the structure of fibrils in situ without the additional preparatory steps needed in the H/D approach.[20] Solid-state NMR is particularly well-suited for examining the structures of smaller fragments of amyloidogenic proteins in detail. If, as here, the fragments are taken from SREs of the parent protein as precursors for inhibitors, ssNMR can easily pinpoint the key

(36) Nagai, Y.; Tucker, T.; Ren, H. Z.; Kenan, D. J.; Henderson, B. S.; Keene, J. D.; Strittmatter, W. J.; Burke, J. R. *J. Biol. Chem.* **2000**, *275* (14), 10437–10442.
(37) Hoshino, M.; Katou, H.; Hagihara, Y.; Hasegawa, K.; Naiki, H.; Goto, Y. *Nat. Struct. Biol.* **2002**, *9* (5), 332–336.
(38) Lu, X. J.; Wintrode, P. L.; Surewicz, W. K. *Proc. Natl. Acad. Sci. U.S.A.* **2007**, *104* (5), 1510–1515.
(39) Carulla, N.; Caddy, G. L.; Hall, D. R.; Zurdo, J.; Gairi, M.; Feliz, M.; Giralt, E.; Robinson, C. V.; Dobson, C. M. *Nature* **2005**, *436* (7050), 554–558.

amyloidogenic residues in the fragments that are candidates for N-methylation or other modification. By relying upon stable isotope labels to report the structural information, ssNMR is also much less invasive than single proline or alanine scanning, for example, which has been used to probe fibril structure by monitoring the effect of mutation on the thermodynamic stability of the fibrils.[40] Proline in particular cannot adopt the correct geometry for a β-sheet and so will grossly alter the peptide conformation, not only locally but also propagating from the substitution site.

In the specific example described here, ssNMR analysis has made a vital contribution toward identifying a peptide, VAQKTmV, that is effective in preventing the aggregation of asyn to form large insoluble fibrillar species as confirmed by DLS and electron microscopy. Several studies have investigated molecules that affect the progression of asyn into insoluble filamentous aggregates, including small organic molecules,[41] antioxidants,[42] β-synuclein,[43,44] and modified peptides based on residues 69−72 of asyn flanked with solubilizing arginine residues.[45] Previous published work has also studied N-methylated variants of peptide fragments derived from residues 69−72 of asyn, but these were not shown to be effective against aggregation of full-length asyn.[46] Our discovery of VAQKTmV as an inhibitor of full-length asyn aggregation has several attractive features: the peptide is small in size, water-soluble, and effective when in equimolar concentration with respect to the target protein. The potential toxic effects of the modified peptide alone and when coincubated with full-length asyn are currently being evaluated, and further work is underway to develop this modified peptide further by optimizing additional druglike properties, such as protease resistance and blood−brain barrier permeability.

Acknowledgment. This work was supported financially with a research fellowship (to J.M, Grant RF2006/3) and equipment grant (Grant 2003B) from the Alzheimer's Research Trust. The BBSRC is acknowledged for funding in support of the 400 MHz NMR facility. Katy Garner carried out some of the preliminary DLS work. The Wellcome Trust is acknowledged for funding the cost of the peptide synthesizer (Grant 075314). Richard Collins is thanked for his assistance with obtaining micrographs.

JA075356Q

(40) Williams, A. D.; Portelius, E.; Kheterpal, I.; Guo, J. T.; Cook, K. D.; Xu, Y.; Wetzel, R. *J. Mol. Biol.* **2004**, *335* (3), 833–842.
(41) Masuda, M.; Suzuki, N.; Taniguchi, S.; Oikawa, T.; Nonaka, T.; Iwatsubo, T.; Hisanaga, S.-i.; Goedert, M.; Hasegawa, M. *Biochemistry* **2006**, *45*, 6085–6094.
(42) Ono, K.; Yamada, M. *J. Neurochem.* **2006**, *97*, 105–115.
(43) Park, J.-Y.; Lansbury, P. T. J. *Biochemistry* **2003**, *42*, 3696–3700.
(44) Hashimoto, M.; Rockenstein, E.; Mante, M.; Mallory, M.; Masliah, E. *Neuron* **2001**, *32*, 213–223.
(45) El-Agnaf, O. M. A.; Paleologou, K. E.; Greer, B.; Abogrein, A. M.; King, J. E.; Salem, S. A.; Fullwood, N. J.; Benson, F. E.; Hewitt, R.; Ford, K. J.; Martin, F. L.; Harriott, P.; Cookson, M. R.; Allsop, D. *FASEB J.* **2004**, *18*, 1315–1349.
(46) Bodles, A. M.; El Agnaf, O. M. A.; Greer, B.; Guthrie, D. J. S.; Irvine, G. B. *Neurosci. Lett.* **2004**, *359* (1−2), 89–93.